Antioxidant Presence in Thick-Walled High-Density Polyethylene Materials After Rotational Molding

Brian L. Weick,[1] Raed S. Al-Zubi[2]

[1]*School of Engineering, University of the Pacific, 3601 Pacific Avenue, Stockton, California 95211*
[2]*National Innovation Center, Poly Processing Company, P.O. Box 80, 8055 South Ash Street, French Camp, California 95231*

Received 22 April 2003; accepted 22 January 2004

ABSTRACT: High-density polyethylene (HDPE) sample tanks manufactured by using a rotational molding process were used in a study to determine the presence and characteristics of antioxidants at the inside and outside surfaces of the tanks. The sample tanks were manufactured by using three different processing times to create undercooked, ideal, and overcooked tanks. Differential scanning calorimetry (DSC) was used to perform oxidation induction time (OIT) studies by using specimens cut from the surfaces of the tank. The OIT portion of the analysis exposes the melted HDPE specimens to an oxygen environment at 200°C for over 2 h. The DSC monitors change in the energy transfer rate to or from the specimen because of chemical reactions. A numerical integration process was used to analyze the DSC-OIT data and to obtain additional information about the energy levels measured during the analysis. Fourier transform infrared (FTIR) studies were also performed to determine the chemical characteristics of specimens cut from the processed tanks. Results showed increased degradation at the inside surfaces of the overcooked tanks because of a lack of antioxidants. The results also showed that metal ions from the mold wall could react with the outside surfaces of the tanks and influence the level of antioxidants at that surface. © 2004 Wiley Periodicals, Inc. J Appl Polym Sci 92: 3052–3066, 2004

Key words: high-density polyethylene; DSC-OIT; antioxidants; rotational molding; phenols

INTRODUCTION

Polyethylene is the most common material used in rotational molding (rotomolding) applications and accounts for more than 85% of the polymers used for this manufacturing process.[1] It is used in a powder form with a 25- to 35-mesh size distribution, and the polyethylene is typically compounded or stabilized with additives such as UV stabilizers and antioxidants.[2] These antioxidants are used to inhibit the degradation of the polyethylene during storage, processing, and end-use applications. The combined effect of elevated temperatures during processing and the presence of oxygen enhances this degradation process, which involves the formation of free radicals within the polymer. Primary antioxidants such as hindered phenols serve to prevent the propagation of these free radicals, and, in turn, prevent the decrease in molecular weight that leads to lower tensile and impact strengths in as-molded products. Further chain branching reactions are also inhibited by the action of secondary antioxidants such as phosphites.

It is well-known that antioxidants serve to prevent degradation from the elevated temperatures experienced during processing.[1,3] This is perhaps the primary reason material suppliers add the antioxidants to commercial polyethylene. However, oxidation can happen during the entire life cycle of a product.[2] Environmental exposure can lead to oxidation as well as exposure to chemicals stored in polyethylene containers. The presence and role of antioxidants after processing is often not considered, and this has not been studied extensively for relatively thick rotomolded commercial products made from high-density polyethylene (HDPE) such as ExxonMobil HD8661 (Houston, TX). In addition, the presence of byproducts from reactions that involve antioxidants has not been studied for the processing conditions used in rotomolding. One technique for determining the level of antioxidants in polymers involves using differential scanning calorimetry (DSC) to perform oxidation induction time (OIT) studies. FTIR studies are also used to gain an understanding of the characteristics of antioxidants and their byproducts.[4]

The determination of the presence and characteristics of antioxidants in relatively thick rotomolded HDPE products represents the overall objective of this study. This includes determining if correlations exist between processing time and antioxidant presence and also includes determining if there is a difference between antioxidant presence at the inside surface of a rotomolded product versus the outside surface. This is

Correspondence to: B. L. Weick (bweick@pacific.edu).

Journal of Applied Polymer Science, Vol. 92, 3052–3066 (2004)

TABLE I
Processing Parameters for Rotomolded Sample Tanks

	Cook cycle				Cool cycle (min)	
Type of tank	Temp. 1 [°C (°F)]	Time 1 (min)	Temp. 2 [°C (°F)]	Time 2 (min)	Fan delay	Fan
Undercooked	274 (525)	12	288 (550)	6	10	15
Ideal	274 (525)	12	288 (550)	10	10	15
Overcooked	274 (525)	12	288 (550)	14	10	15

important because different thermal and environmental conditions exist for inside surfaces of an HDPE product that are formed last during the rotomolding process when compared to outside surfaces of a product that are formed first on the mold wall. Although there are limitations to using DSC-OIT measurements to make direct, quantitative predictions about long-term thermal or processing stability of polyolefins, the technique is sound for determining the presence of phenolic antioxidants using samples taken from various surfaces of rotomolded HDPE products.[5,6] Therefore, DSC-OIT will be used to study the thermal degradation characteristics of rotomolded HDPE sample products fabricated under controlled conditions. FTIR will also be used to study the sample products as needed. Cube-shaped tanks with a nominal 6.4 mm (0.25 in.) thickness were chosen as these sample products, and three types of tanks were rotomolded by using different processing times. Undercooked and overcooked tanks were rotomolded in addition to ideal tanks that were manufactured by using the normal processing time. Samples from inside and outside surfaces of the rotomolded tanks were studied, and comparisons were made to gain insight into the degradation and antioxidant characteristics of rotomolded HDPE products.

EXPERIMENTAL

Test equipment

An Instrument Specialists Inc. DSC 550 (Spring Grove, IL) was used to run all of the differential scanning calorimetry experiments. Calibration for this instrument was performed by using the indium and zinc standards. In addition, the DSC was connected to oxygen and nitrogen tanks through control valves. Experiments could then be run in pure nitrogen or pure oxygen environments. Weight measurements were obtained by using a Mettler A240 balance (Toledo, OH). Fourier transform infrared (FTIR) studies were performed by using a Shimadzu FTIR 8300 spectrophotometer operating in transmission mode (Columbia, MD).

Test samples

An STP Lab 40 shuttle-type rotational molding machine was used to fabricate cube-shaped tanks with a nominal 6.4 mm (0.25 in.) wall thickness (STP Equipment Inc., Bromptonville, Quebec, Canada). Exterior dimensions for the tanks were 0.3 × 0.3 × 0.3 m (12 × 12 × 12 in.). The mold was fabricated from stainless steel (SST), and a 4 : 1 rotation ratio was used between the major and minor axes during the rotomolding process. The flat-sided cube-shaped tanks were used as a source of test specimens for the analytical study. A plane was used to extract 0.76-mm (0.030-in.)-thick shavings from the flat panels, and 4.0-mm (0.16-in.)-diameter test specimens were punched out by using a hole punch. Test specimens were weighed by using a Mettler balance, and specimen masses varied from 8 to 11 mg. The standard specimen size and mass were used throughout the study to minimize imprecisions in OIT/DSC results that could be attributed to inconsistent sample preparation.[7,8] Processing parameters for the three tanks are listed in Table I. Note that the Cook Cycle consisted of two time periods. The first time period at 274°C was 12 min for all three tanks, and the second time period at 288°C was 6 min for the undercooked tank, 10 min for the ideal tank, and 14 min for the overcooked tank. The temperatures and time periods for the ideal tank represent standard rotational molding parameters for processing of HDPE tanks by the Poly Processing Co.

Experimental procedures

ASTM D3895 was used as the guideline for running the DSC-OIT experiments. The 4.0-mm-diameter test sample was first placed in an open DSC pan after it was weighed. The sample was then placed in the DSC next to the reference pan, which was an empty DSC pan of known weight. After closing the chamber, nitrogen flowing at a rate of 5 mL/min was used to purge the chamber for a period of 5 min. Once this 5-min period was complete, the DSC was started. The experiment was performed in two segments as shown in Table II, and Figure 1 shows a typical data set acquired by using this procedure. The first segment was performed in a nitrogen environment with nitrogen flowing at 5 mL/min. The initial temperature of the chamber was at approximately 25°C or slightly lower depending on ambient temperature conditions. The temperature was then increased at a rate of 20°C per minute until a final temperature of 200°C was reached. During this first segment, the sample passed

TABLE II
DSC Settings Used for OIT Experiments

	Start temp. (°C)	End temp. (°C)	Heating rate (°C/min)	Hold time (min)	Gas type
Segment 1	25	200	20	5	Nitrogen
Segment 2	200	200	20	140	Oxygen

Sample rate = 1 sample/s.

through an endothermic glass transition prior to reaching 50°C. A large endothermic peak that occurred at ~137°C corresponds with the crystalline melting point for the polyethylene material. After the sample passed through this melting point, it was in a liquid state. Once the DSC reached a temperature of 200°C, the 5-min hold period began. Because the temperature was no longer being increased, the rate of energy transfer returned to ~ 0. As shown in Figure 1, when the 5-min hold period was complete, segment 1 ended and segment 2 began. The nitrogen valve was turned off, and the nitrogen was allowed to bleed from the chamber until the flow rate was 0 mL/min. At this point, the oxygen valve was turned on, and oxygen was allowed to flow into the chamber at a rate of 5 mL/min. This was the starting point for the OIT experiment, and the experiment was allowed to run for 140 min in the oxygen environment. Note that Figure 1 shows typical results for the initial part of an OIT experiment from 0 to 0.20 h.

FTIR samples were obtained by using a razor knife to slice samples from surfaces of the tanks. These samples were approximately 10 mm in diameter. They were held in the chamber by using standard fixtures for the Shimadzu FTIR 8300, which was operated in transmission mode.

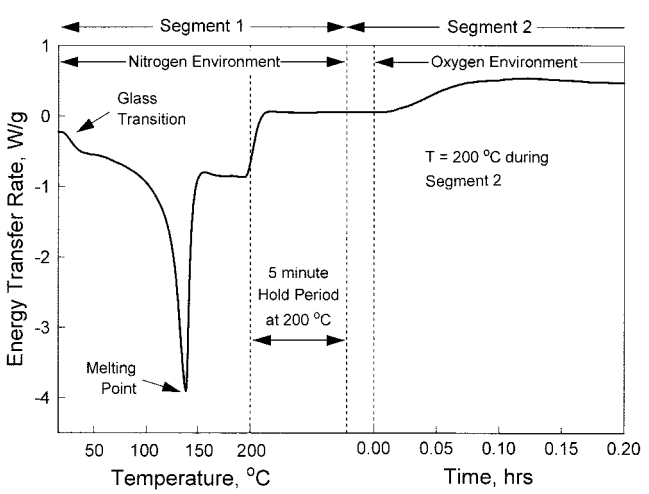

Figure 1 Typical results for a differential scanning calorimetry–oxidation induction time (DSC-OIT) experiment. Segment 1 represents the temperature-controlled part of the experiment in which the sample is melted in a nitrogen environment. The first 0.2 h of segment 2 is shown, and this segment is performed at a 200°C temperature for 140 min (2.3 h) in an oxygen environment.

AUTOXIDATION AND STABILIZATION OF POLYETHYLENE

Autoxidation

The characteristics of antioxidants used to stabilize polymers for end-use applications have been reviewed quite extensively in the literature. Gugumus[4] and Zweifel[9] provide excellent reviews of the types of antioxidants and their function in specific polymers. The kinetics of antioxidant behavior are described by Shlyapnikov et al.,[10] and a review of the chemical activity of polymer stabilizers is provided by Pospisil and Nespurek.[11]

The reaction of polymers with molecular oxygen yields oxidation products and breakdown of the polymer chain. It is a free-radical-initiated process that proceeds autocatalytically. The process involves initiation, propagation, and termination reactions that have been discussed by Gugumus[4] and Zweifel.[9] The origin of the primary alkyl radicals R· that initiate the autoxidation reaction can be attributed to a number of factors. They are initially formed during polymer synthesis due to the presence of residual catalysts such as transition metals, radical initiators, and other impurities. However, the pertinent radical formation mechanism for rotomolding is the thermomechanical degradation process that involves high mechanical forces when the polymer molecules become entangled during processing. This leads to C—C chain scission resulting in the formation of alkyl radicals R· and a simultaneous reduction of molecular weight.[9] Additional alkyl radicals are formed during the chain propagation steps described below, but the formation of alkyl radicals that serve as initiators for the autoxidation process cannot be prevented and is summarized in eq. (1).

Chain initiation due to alky radical R· formation

$$\text{R-H} \quad \text{or} \quad \text{R-R} \longrightarrow \text{R}\cdot \tag{1}$$

where R represents the polymer chain.

With the presence or introduction of oxygen, it is conceivable that more alkyl radicals R· will be produced. However, this reaction is considered to be unfavorable due to thermodynamic and kinetic considerations.[4,9] Instead, the presence or introduction of oxygen leads to the generation of peroxy radicals ROO· and further breakdown of the macromolecular chain as described by eqs. (2) and (3).

Chain propagation due to presence or introduction of oxygen

$$R\cdot + O_2 \xrightarrow{k_1} ROO\cdot \quad (2)$$

$$ROO\cdot + RH \xrightarrow{k_2} ROOH + R\cdot \quad (3)$$

The activation energy for eq. (2) is minimal; therefore, the peroxy radicals ROO· are produced rapidly when alkyl radicals R· are exposed to oxygen. These peroxy radicals can then react with the polymer chain RH, causing the formation of hydroperoxides ROOH and more alkyl radicals R·, as shown by eq. (3). This reaction leads to the breakdown of the polymer, and the rate of this reaction is generally regarded as the critical rate for oxidation. Other propagation reactions can and do occur as described by Gugumus[4] and Zweifel.[9] Further chain branching reactions can occur due to the breakdown of the hydroperoxides into alkoxy and hydroxy (RO· and ·OH) radicals. These radicals can in turn lead to further chain propagation or generation of more peroxy ROO· radicals in the presence of sufficient oxygen.[4] In addition, it is important to note that the hydroperoxides can also decompose to alkoxy, peroxy, and hydroxy radicals under the influence of metal ions at elevated temperatures, as shown by eqs. (4) and (5):

$$M^{n+} + ROOH \rightarrow M^{(n+1)} + RO\cdot + HO^- \quad (4)$$

$$M^{(n+1)} + ROOH \rightarrow M^{n+} + ROO\cdot + H^+ \quad (5)$$

Chain termination will eventually occur once the initiation, propagation, and branching steps have taken place. However, by this time the molecular weight of the polymer has decreased, and the mechanical characteristics have been diminished. Therefore, prevention of the autoxidation process is primarily achieved by adding stabilizers to inhibit the chain propagation reaction. These primary stabilizers convert the emerging radicals to stable end-products. Secondary stabilizers are also added to convert intermediate products such as the hydroperoxides to stable end-products.

Stabilization of polyethylene using antioxidants

Chemists have developed antioxidants that interfere with the propagation process described by eq. (3). The formation of alkyl radicals R cannot be avoided because of the thermomechanical manner in which they are formed. The generation of peroxy radicals ROO is also unavoidable due to the extremely high reaction rate between the alkyl radicals R and oxygen. Therefore, antioxidants were developed that can react with the peroxy radicals and form a stable, nonradical product. General reaction equations that describe the action of antioxidants are shown in eqs. (6) and (7)[4,9]:

$$ROO\cdot + AH \xrightarrow{k_a} ROOH + A\cdot \quad (6)$$

$$ROO\cdot + A\cdot \xrightarrow{k_b} A\text{-}OOR \quad (7)$$

In this chain-breaking donor mechanism (CB-D) the peroxy radical ROO extracts a hydrogen atom from the primary antioxidant AH, which causes the formation of hydroperoxides and an antioxidant radical A·. This antioxidant radical can then react with additional peroxy radicals to form a stable end-product, which can be depicted in general as A-OOR.

Phenols are currently the most common type of primary antioxidant used for polyethylene. The basic mechanism follows the general reactions shown in eqs. (6) and (7), and a more detailed depiction of these reactions is shown in eqs. (8) and (9).[4,9] Note that the R^1 and R^2 groups shown in these equations can be either H, methyl, or *t*-butyl groups, and R^3 can be a *t*-butyl group. However, Pospisil and Nespurek[11] have noted that other functional moieties can be used for R^3, including additional aromatic rings, ester groups, sulfides, phosphonates, oxamides, and compounds containing various forms of triazines. The steric hindrance of the R^1 and R^2 groups controls the rate of H extraction from phenol, which decreases when the steric hindrance increases. As shown in eq. (8a), the antioxidant radical that forms because of H extraction is a phenoxy radical with the unbonded electron associated with the oxygen atom. This structure is quasi-stable, and eq. (8b) shows that carbonyl groups tend to form with a change in the location of the unbonded electron. The more complex R^3 group is likely to play a role in this reaction because of the increased electron withdrawing characteristics of the group

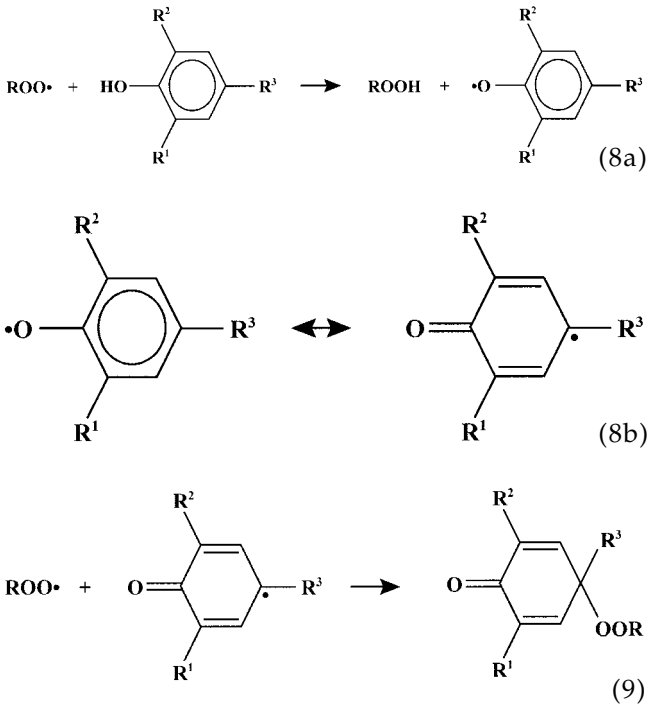

Although the reactions shown in eqs. (8) and (9) are more detailed than those shown in eqs. (6) and (7), they are still rudimentary at best. Equations (8) and (9) depict the general action of hindered phenols. In his recent review, Zweifel[9] noted that sterically hindered phenols currently used for commercial purposes have a propionate group for R^3. In general, this can lead to two types of stable reaction products. One takes the form of the reaction product shown in eq. (9) due to reaction with the peroxy radical and contains the carbonyl group in the aromatic ring with the propionate group substituted for R^3. The other stable product is a C—C coupled product that does not contain the carbonyl groups in the aromatic ring. Pospisil and Nespurek[11] have also discussed the formation of these stable products along with the quinone methides that can in turn react with alkyl radicals, peroxy radicals, and hydrogen peroxide groups to form stable products.

Additional types of antioxidants include those that participate in the chain breaking acceptor (CB-A) mechanism discussed by Gugumus.[4] This mechanism plays a role when processing conditions exclude oxygen. Secondary antioxidants such as phosphites also play a role. The phosphites prevent the hydroperoxides from being converted into alkoxy and hydroxy radicals. Zweifel[9] points out that the phosphites are consumed during processing conditions and are rapidly converted to phosphates. Therefore, the long-term stability of the polymer depends on the phenol concentration. Recently, thiosynergists have also been blended with the polymer and phenol antioxidants, and these have also imparted a significant improvement in thermooxidative stability.[9] In addition, sterically hindered amines have been proposed as possible stabilizers; however, the phenol + phosphite combination appears to be the preferred combination for processing of polyolefins such as polyethylene.[9]

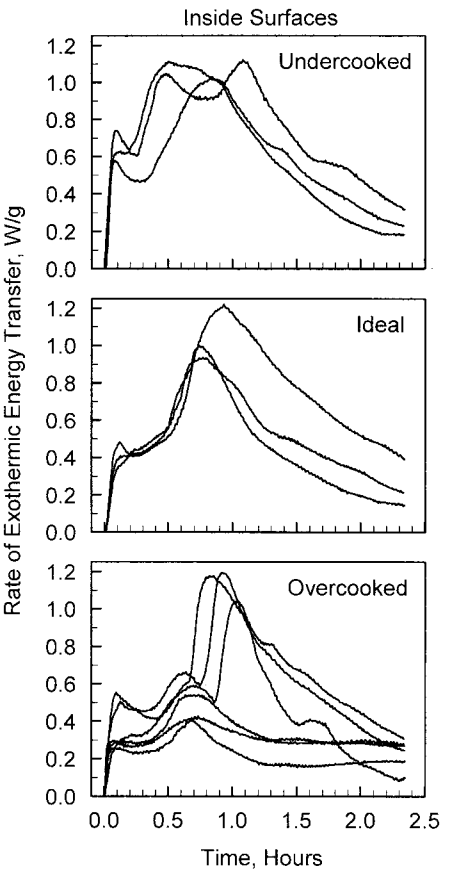

Figure 2 Exothermic energy transfer rates for samples from the inside surfaces of three rotomolded tanks.

RESULTS AND DISCUSSION

Exothermic energy transfer rates

Results from DSC-OIT experiments are shown in Figures 2 and 3. These figures show exothermic energy transfer rates for samples taken from the inside and outside surfaces of the three test tanks: undercooked, ideal, and overcooked. A time of 0 h corresponds to the point when oxygen is introduced into the test chamber. This occurs after the sample has been heated up to 200°C in a nitrogen environment during the initial temperature-controlled phase of the experiment and stabilized for 5 min at that temperature. The temperature is maintained at 200°C when oxygen is introduced at time 0, and changes in the rate of exothermic energy transfer from the polymer sample are monitored by using the DSC for 140 min (2.3 h). The exothermic energy transfer rate is normalized with respect to the weight of the sample and is in units of

Watts per gram. Three repeat experiments were performed for each of the sample types; however, six repeat experiments were performed by using samples from the inside surface of the overcooked tank to establish trends. Within the first 0.02 h, all the samples passed through an initial peak followed by a slight decrease in energy transfer rate, although some of these peaks manifest themselves as shoulders in the curves followed by a leveling-off period. Final peaks in the energy transfer rate occur after 0.5 to 1.5 h followed by a gradual decrease until the end of the experiment. It is important to note that Figure 2 shows the occurrence of two distinct final degradation peaks for samples from the inside surface of the overcooked tanks, which corresponds with distinct quasi-stable degradation products for these samples. Two final degradation peaks were also observed for one of the samples shown in Figure 2 from the inside surface of the undercooked tank. However, this double peak is due to the presence of two anomalous melting zones that formed for this particular sample.

To facilitate the understanding of the initial part of the DSC-OIT experiments, the exothermic energy transfer rates shown in Figures 2 and 3 are replotted for a shorter 0.25-h time period in Figures 4 and 5. Based on the ASTM definition of oxidation induction time, the OIT is less than 0.02 h for all the samples, which is indicative of significant antioxidant consumption during processing. However, in addition to measuring the OIT, it is perhaps more important to understand the reaction mechanisms and corresponding energy transfers that occur during the degradation process rather than just the time it takes to initiate the process. Shylapnikov et al.[10] stated that the induction period could be regarded as the rate we consider to be complete. Knowledge gained from the DSC-OIT experiments cannot only lend insight into the degradation reactions that occur for the HDPE tanks due to processing and environmental exposure, but this knowledge can also show how antioxidant presence is a function of part thickness and processing time.

A general depiction of the degradation process experienced by the polymer samples during the DSC-OIT experiments is shown in Figure 6. All of the samples experienced the general trend depicted in Figure 6 with differences in peak heights, times, and widths, although samples from the inside surface of the overcooked tank exhibited different characteristics that will be discussed in a later section of this article.

During the initial part of the experiment shown as time period I in Figure 6, the polymer experiences a rapid increase in exothermic energy transfer rate. This rapid increase occurs shortly after the introduction of oxygen into the chamber and is likely to correspond to chain propagation reactions as well as antioxidant radical formation. Recall that alkyl radicals R have been generated during the rotomolding process due to thermomechanical degradation and are already present in the polymer prior to beginning the DSC experiment. The sample is melted in a nitrogen environment during the temperature-controlled portion of the experiment and then held for 5 min in this environment at 200°C. At this point, the nitrogen is purged from the chamber, and oxygen is introduced corresponding to time 0 in Figures 2–6. Once this oxygen is introduced, the alkyl radicals R react very rapidly with the oxygen to form the peroxy radicals ROO·. This is shown in eq. (2), and the reaction rate, k_1, is very fast and uncontrollable.[9] The peroxy radicals are subsequently consumed in one of two manners. They are either used in the oxidation reaction shown in eq. (3) or used to generate antioxidant radicals, as shown in eq. (6). Recall that the oxidation reaction involves breakdown of the polymer chain through hydrogen extraction to form hydrogen peroxide and more alkyl radicals. Equation (3) is the rate-determining equation for oxidation and occurs at a reaction rate k_3. Antioxidant radicals produced at a rate of k_a, shown in eq. (6), can scavenge these peroxy radicals according to eq. (7) and prevent the chain breakdown represented by eq. (3). However, k_a must be greater than k_3 or the stabilization action of the antioxidants represented by eq. (7) will not work.[9]

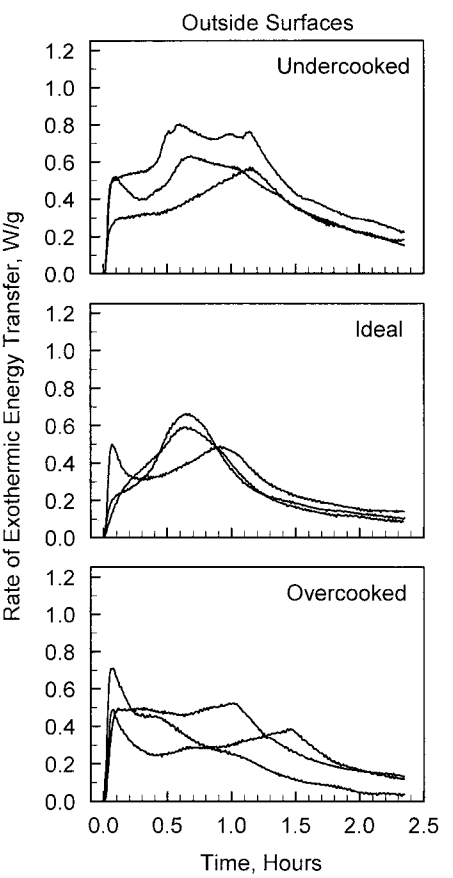

Figure 3 Exothermic energy transfer rates for samples from the outside surface of three rotomolded tanks.

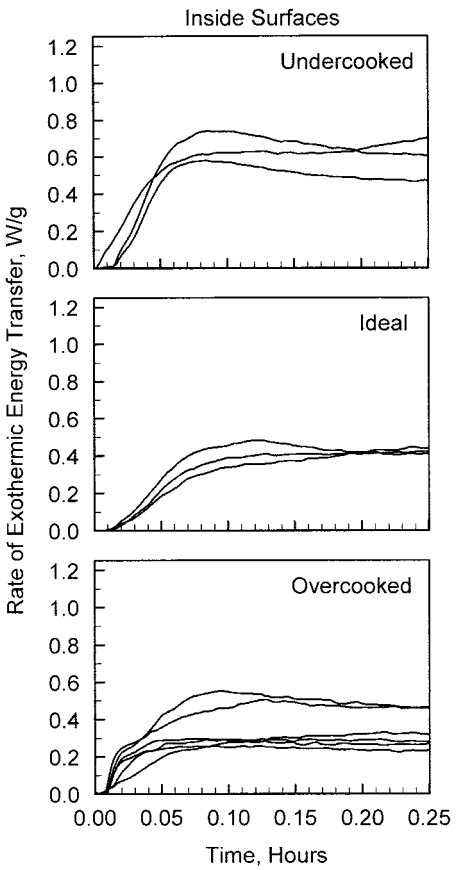

Figure 4 Exothermic energy transfer rates for samples from the inside surfaces of three rotomolded tanks. Initial 0.25 h.

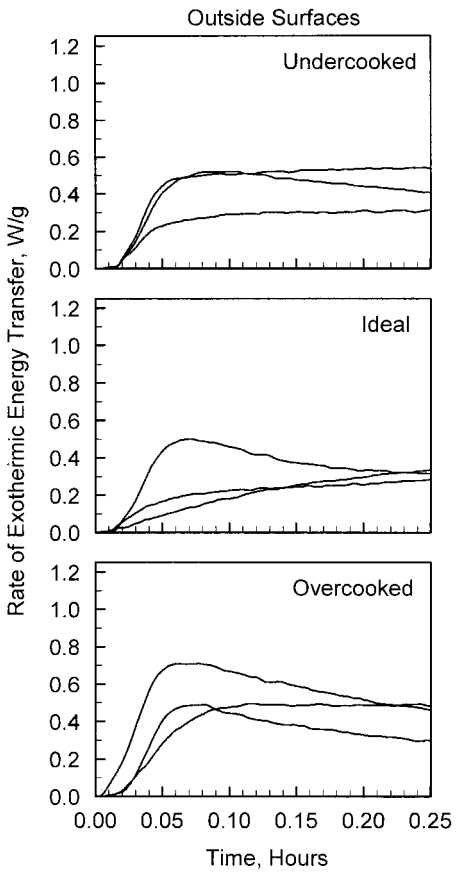

Figure 5 Exothermic energy transfer rates for samples from the outside surface of three rotomolded tanks. Initial 0.25 h.

The initial time periods in Figures 2–5 follow the general trends depicted in Figure 6 for time period I. After the very short (<0.02 h) induction period, the oxygen concentration is high enough to react with the alkyl radicals according to eq. (2) at the high exothermic reaction rate of k_1. This occurs along with polymer chain breakdown at a rate of k_3 as well as antioxidant radical generation at a rate of k_a according to eqs. (3) and (6), respectively. As a result, the exothermic energy transfer accelerates until a significant number of alkyl radicals R have been consumed and the antioxidant radicals have reached a significant concentration level to begin reacting with the peroxy radicals ROO to form nonradical end-products according to eq. (7), and therefore, prevent chain propagation.

Once the antioxidant radicals begin scavenging the peroxy radicals, the exothermic energy transfer rate reaches a peak, and either decreases or levels off as shown in Figure 6. This decrease or leveling-off occurs in time period II and represents the antioxidant reactions [eqs. (6) and (7)], canceling out the chain propagation reaction [eq. (3)[rsqb]. Peroxy radicals are scavenged by the antioxidant radicals to produce stable end-products. However, once the antioxidants have been consumed, the chain propagation reaction can proceed in an uninhibited manner. This occurs during time period III and corresponds with a final acceleration in exothermic energy transfer until a peak level is reached and terminal reactions cause the rate of energy transfer to decrease. Note that some samples shown in Figures 2 and 3 exhibit rather sharp peaks in

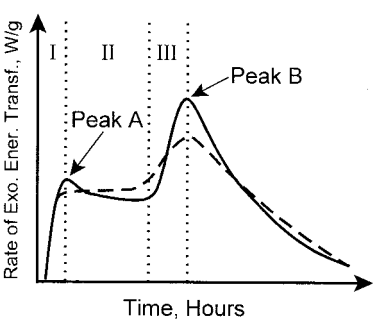

Figure 6 General depiction of degradation curves. Time periods I, II, II are shown along with characteristic Peaks A and B reached during the degradation process. Solid lines and dashed lines show typical shapes for the degradation curves.

time period III, whereas others exhibit broader peaks. These general trends are shown by the solid and dashed lines in Figure 6.

Integrated energy transfer rates

Integration process

The time it takes for the antioxidants to activate and begin inhibiting the autoxidation reactions can be measured by using the DSC-OIT results shown in Figures 2–5. Final degradation time can also be measured by using these results. In addition, the energy dissipated during these time periods can be quantified by integrating these curves from time 0 out to the peaks in energy transfer rate. The methodology for quantifying the results is shown in Figure 6. Peak A represents the time it takes for the antioxidants to activate and begin the inhibition process, and the integrated area from time 0 to this peak represents the energy transfer during this time period in Joules per gram. Peak B represents the time it takes for the energy transfer rate associated with final degradation to reach a maximum. Integrating the area under the curve to Peak B represents the amount of energy dissipated at the point when the degradation rate reaches a maximum. Data shown in Figures 4 and 5 for the 0- to 0.25-h time period were used to determine the location of Peak A, whereas data shown in Figures 2 and 3 were used to determine the location of Peak B. (In some cases where the peaks were notably broad, Peak B maximums were considered to be the points where the data sets showed significant decreases after reaching a maximum level.) Simpson's rule for numerical integration was used to integrate the exothermic energy transfer rates from time 0 out to Peak A or Peak B. This allowed for the integrated exothermic energy transfer curves to be plotted as a function of time in Figures 7-10.

Results from integration process

Exothermic energy transfer curves for the initial reactions are shown in Figures 7 and 8 for samples from the inside and outside surfaces of the undercooked, ideal, and overcooked tanks. These curves were developed by integrating the energy transfer rate curves in Figures 4 and 5 out to Peak A. Energy and time scales in Figures 7 and 8 are kept the same for the three test tanks, and an inset for the overcooked tank in Figure 7 provides more detailed information at reduced energy and time scales. Error bars shown in Figures 7 and 8 are confidence intervals calculated by using standard deviations for replicate data sets and values from the Student t probability distribution function. By integrating the curves and plotting them on a shorter time scale, it is easier to get a more

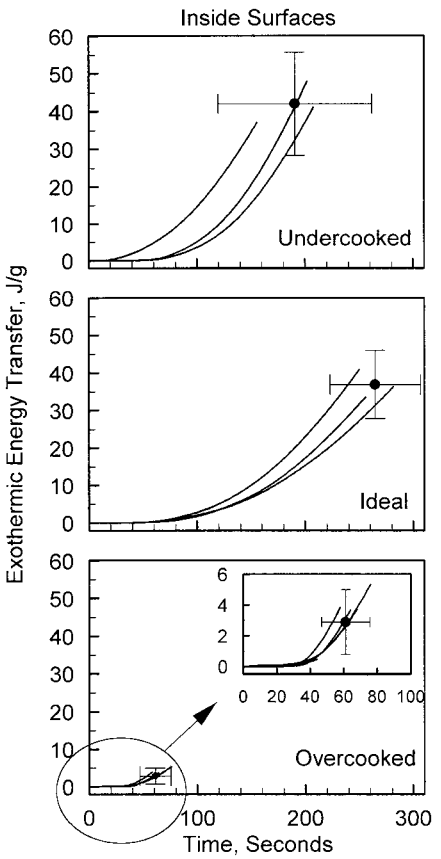

Figure 7 Integrated energy transfer curves for samples from the inside surfaces. Initial 300 s. Data points indicate average values for Peak A.

accurate estimation of the OIT as defined by ASTM. This entails determining when the initial reactions begin to increase from a zero energy level. As shown in Figure 7, oxygen is introduced at time 0, and initial reactions for the inside surface of the overcooked tank start to increase after only 40 s. In comparison, initial reactions for samples from the inside surfaces of the ideal and undercooked tanks begin after approximately 70 s with one replicate experiment for the undercooked tank initiating at around 20 s. Samples from the outside surfaces of the tanks also have an induction period of approximately 70 s, although one replicate experiment for a sample from the outside surface of the overcooked tank has a lower induction time. Based on these experiments, it can be stated that samples from the inside surface of the overcooked tank undergo the shortest induction period of approximately 40 s, which is consistent with increased antioxidant consumption due to a longer processing time and exposure to air in the mold. However, this is not the only statement that should be made using these data sets. More information can be obtained in addition to the OIT values.

The exothermic energy transfer curves in Figures 7 and 8 are nonlinear, which shows that the rates of the

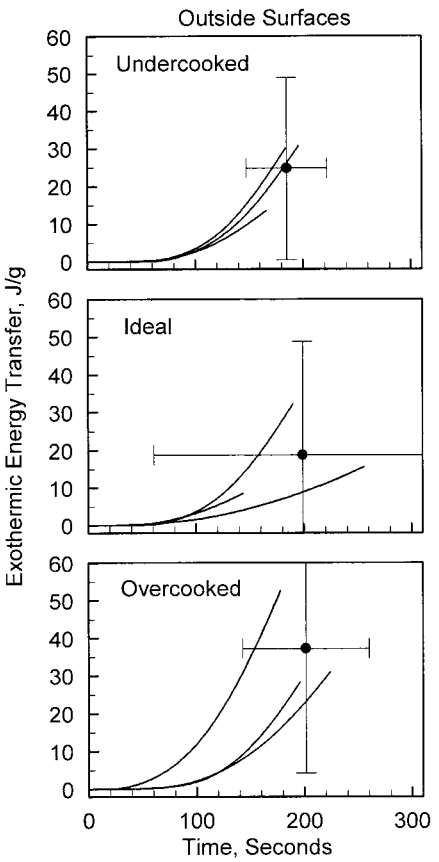

Figure 8 Integrated energy transfer curves for samples from the outside surfaces. Initial 300 s. Data points indicate average values for Peak A.

reactions are increasing during the experiments. Furthermore, recall that initial reactions correspond with alkyl radicals reacting with oxygen to produce peroxy radicals [eq. (2)[rsqb] followed by reaction between the polymer chain and the peroxy radicals resulting in breakdown of the polymer [eq. (3)[rsqb]. At the same time, antioxidant radicals are being produced by reaction between the peroxy radicals and the antioxidant [eq. (6)[rsqb]. The maxima in Figures 7 and 8 correspond to points where the antioxidant radicals begin to scavenge the peroxy radicals and produce stable end-products according to eq. (7). This occurs very quickly for samples from the inside surface of the overcooked tanks and corresponds with a lower exothermic energy transfer when compared to the ideal and undercooked tanks. This is consistent with antioxidant and radical consumption during the rotomolding process. Therefore, the remaining antioxidant levels are lower for the inside surface of the overcooked tank. Visual inspection of Figure 7 shows that the energy levels at peak A for the undercooked and ideal tank are somewhat higher than the levels measured for the overcooked tank. This is again consistent with more antioxidant consumption during processing for the overcooked tank when compared to the undercooked and ideal tanks. This general trend is also observed for the time required to reach Peak A, and the time for samples from the inside surface of the overcooked tank is certainly less than the time for the undercooked and ideal tanks. However, samples from the inside surface of the ideal tank appear to reach Peak A more slowly than samples from the undercooked tank. It is unclear why this occurs, although trapped air in the undercooked tank sample after processing could play a role not only in decreasing the amount of time for the initial reactions to occur, but also in decreasing the amount of time for the antioxidant radical levels to build up and begin scavenging the peroxy radicals. From Figure 8, Peak A maxima for outside surface samples show a great deal of spread, and a statistical comparison will be presented by using an analysis of variance (ANOVA) when results shown in Tables III and IV are discussed.

Recall from the general description of the degradation process shown in Figure 6 that a decrease or leveling-off period follows the initial reactions that occur in time period I. Once Peak A is reached, the

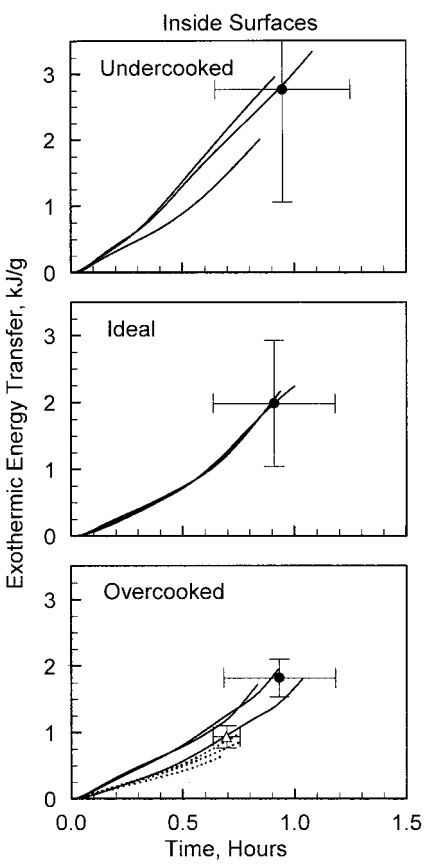

Figure 9 Integrated energy transfer curves for samples from the inside surfaces. Circular data points indicate average values for Peak B. Dashed lines show integrated curves for degradation process experienced by certain overcooked tank samples. Triangular data point indicates average value for Peak B′.

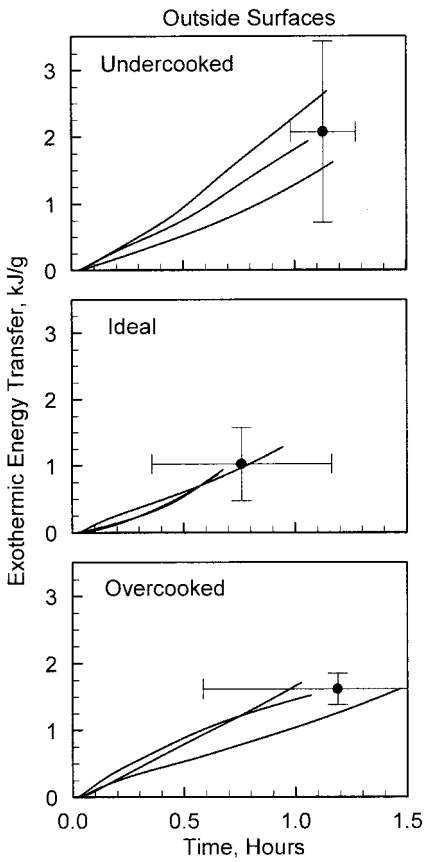

Figure 10 Integrated energy transfer curves for samples from the outside surfaces. Circular data points indicate average values for Peak B.

level of antioxidant radicals has increased to the point where peroxy radicals can be scavenged, preventing further chain breakdown. This continues during time period II in Figure 6, until the antioxidant radicals are consumed. At this point, the propagation reaction shown in eq. (3) can occur in an uninhibited fashion as shown by time period III in Figure 6. This causes a rapid increase in the rate of exothermic energy transfer, which reaches a maximum at Peak B. To gain insight into this process, the energy transfer rate curves shown in Figures 2 and 3 were integrated from time 0 out to Peak B. These integrated curves are presented in Figures 9 and 10 for the inside and outside surfaces, respectively. Energy transfer in kJ/g is shown as a function of time in hours. Replicate experiments for each tank type are shown along with error bars corresponding with confidence intervals for the maximum energy levels and time to reach Peak B. In Figure 9, an additional set of dashed curves is shown for the sample from the inside surface of the overcooked tanks. These dashed curves represent different peaks that occurred for this sample, and either occurred as additional peaks before Peak B or were the final peaks measured for the sample. Two of the six replicate experiments from Figure 2 are shown alone in Figure 11 to show the differences between the two types of experiments. The additional peaks are labeled as Peak B′. Curves shown as dashed lines in Figure 9 were obtained by integrating the energy transfer rate data from time 0 out to a maximum represented by Peak B′. As presented in a later section of this article, FTIR analysis provides some possible explanations for the existence of the quasi-stable Peak B′.

Comparison of results based on processing time

To facilitate making comparisons between the DSC-OIT data obtained for the undercooked, ideal, and overcooked tanks, the data sets from Figures 7 and 8 are superimposed on one another in Figure 12. Similarly, data sets from Figures 9 and 10 are superimposed in Figure 13. (Note that the curves corresponding to Peak B′ are not shown in Fig. 13.) Data sets shown in Figure 12 depict the energy levels during the initial 300 s of the experiments for both the inside and the outside surfaces of the three tanks, and data sets in Figure 13 show energy levels during the experiment out to the final degradation point at Peak B. Analytical comparisons between the data sets can then be made by using a one-way ANOVA. This statistical technique

TABLE III
Peak Energy Levels and Time-to-Peak for HDPE Samples (Comparison of Values for Undercooked, Ideal, and Overcooked Samples using One-way Analysis of Variance)

		Sample tank			Pooled standard deviation	Statistics one-way analysis of variance		
	Surface	Undercooked	Ideal	Overcooked		*F* value	*P* value	Probability, (%)
Energy levels peak A (J/g)	Inside	42	37	3	4	170	0.00	100
	Outside	25	19	37	12	2	0.23	77
Time-to-peak A (s)	Inside	191	265	61	19	131	0.00	100
	Outside	185	199	201	36	0.2	0.84	16
Energy levels peak B (kJ/g)	Inside	2.8	2.0	1.8	0.5	3.7	0.09	91
	Outside	2.1	1.0	1.6	0.3	7.0	0.03	97
Time-to-peak B (h)	Inside	1.0	0.9	0.9	0.1	0.1	0.91	9
	Outside	1.1	0.8	1.2	0.2	5.5	0.04	96

TABLE IV
Peak Energy Levels and Time-to-Peak for HDPE Samples (Comparison of Values from Inside and Outside Surfaces using One-way Analysis of Variance)

	Sample tank	Inside surface	Outside surface	Pooled standard deviation	Statistics one-way analysis of variance		
					F value	*P* value	Probability (%)
Energy levels peak A (J/g)	Undercooked	42	25	8	7.2	0.06	94
	Ideal	37	19	9	6.2	0.07	93
	Overcooked	3	37	7	45	0.00	100
Time-to-peak A (s)	Undercooked	191	185	23	0.1	0.77	23
	Ideal	265	199	41	3.8	0.12	88
	Overcooked	61	201	17	134	0.00	100
Energy levels peak B (kJ/g)	Undercooked	2.8	2.1	0.6	1.9	0.25	75
	Ideal	2.0	1.0	0.3	14	0.02	98
	Overcooked	1.8	1.6	0.1	5.7	0.08	92
Time-to-peak B (h)	Undercooked	1.0	1.1	0.1	5.4	0.08	92
	Ideal	0.9	0.8	0.1	1.7	0.26	74
	Overcooked	0.9	1.2	0.2	2.9	0.17	83

evaluates whether or not the energy levels or time-to-peak values are significantly different. Table III provides results from the one-way ANOVAs performed to compare results for the undercooked, ideal, and overcooked tanks. Average energy levels and time-to-peak values for Peak A and Peak B are also shown in Table III for the inside and outside surfaces of the three tanks. Note that the one-way ANOVA uses a pooled standard deviation that assumes the type of error is the same for each of the experiments, regardless of whether or not an undercooked, ideal, or overcooked tank sample is being tested. Values of these pooled standard deviations are also shown in Table III and provide some insight into the overall spread to the data. Statistics for the one-way ANOVA include the *F* value from the evaluation as well as the *P* value. High *F* values and low *P* values correspond with high probability that the data sets are significantly different. The probability value shown in the last column was determined by subtracting the *P* value from 1.00 and multiplying the results by 100. Therefore, a *P* value of 0.23 corresponds to a 77% probability, and a *P* value of 0.00 corresponds to a 100% probability.

The first row in Table III shows results for samples from the inside surface of the three tanks. Peak A

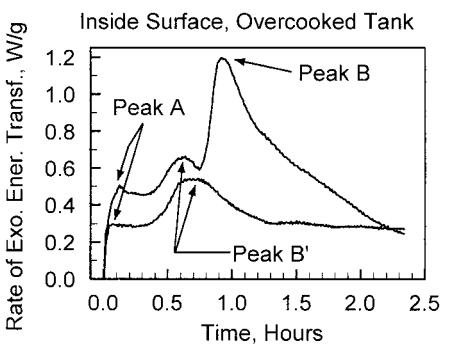

Figure 11 Typical degradation curves for samples from the inside surface of the overcooked tank. Characteristic peaks in the energy transfer rates are labeled as Peaks A, B, and B′.

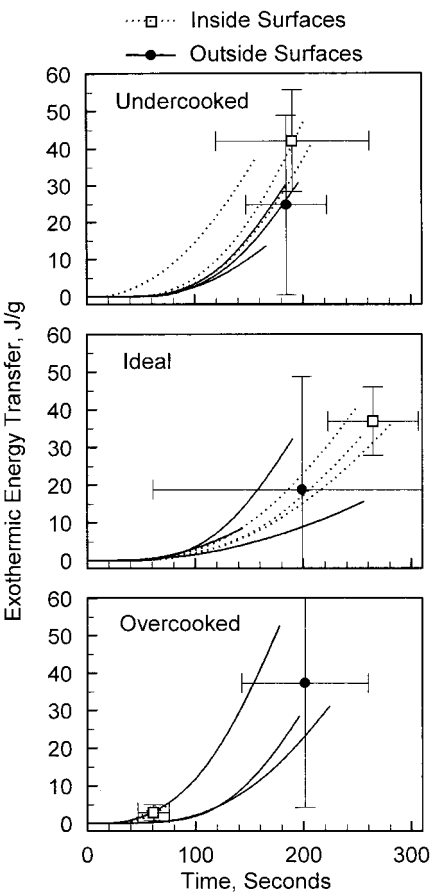

Figure 12 Comparison of integrated energy transfer curves for samples from the inside and outside surfaces. Initial 300 s. Data points indicate average values for Peak A.

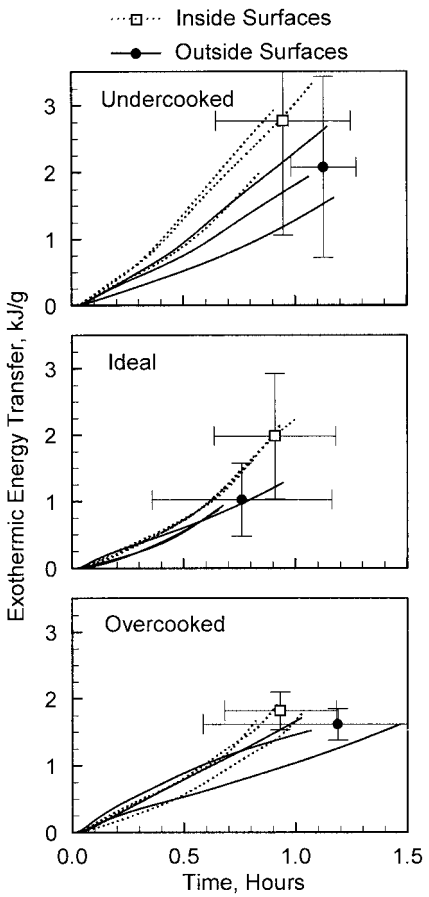

Figure 13 Comparison of integrated energy transfer curves for samples from the inside and outside surfaces. Data points indicate average values for Peak B.

energy levels are compared, and the one-way ANOVA shows that there is a 100% probability that the values are different. Furthermore, the energy levels at Peak A decrease with processing time, with the overcooked tank having the lowest energy level. This corresponds with a lower amount of antioxidant at the inside surface of the overcooked tank, and therefore, a lower amount of energy is required to form the antioxidant radicals [eq. (6)[rsqb] and begin scavenging the peroxy radicals [eq. (7)[rsqb] formed by alkyl radicals reacting with oxygen. Time-to-Peak A values also show a significant difference for samples from the inside surface, and the overcooked tank reaches this peak in the shortest time. Once again, this supports the argument for antioxidant reduction. However, samples from the inside surface of the ideal tank appear to take longer than samples from the undercooked tank to reach Peak A. This is possibly due to increased levels of air absorbed in the undercooked tank that could have led to increased radical generation and consumption of antioxidants during the rotomolding process.

Samples from the outside surface of the three tanks show energy levels corresponding to Peak A that have only a 77% probability of being different. This is not considered to be significant by normal standards established for statistical comparison. Typically, 90, 95, or >99% probabilities are considered to be the normal measurements for significance. Time-to-Peak A values for the outside surface of the tanks are definitely not different, with a P value of 0.84 and a probability of only 16%. In fact, with such a low probability, one can argue the reverse hypothesis that states the time-to-Peak A values are the same for the outside surface of the overcooked tank. From this information, it can be proposed that the energy levels and time-to-Peak A values for the outside surfaces are not as greatly affected by processing time as the values for the inside surface. This supports the likelihood of increased antioxidant consumption during the rotomolding process at the inside surface as well as a corresponding increase in consumption of free alkyl radicals because of peroxy radical formation and subsequent scavenging by the antioxidant radicals. Such a process should result in the formation of carbonyl groups after the overcooked tanks have been processed, which is confirmed by the FTIR results discussed in a later section of this article.

Average energy levels required to reach Peak B are also shown in Table III along with time-to-Peak B values. The difference between Peak B energy levels appears to be significant when values for the undercooked, ideal, and overcooked tanks are compared by using samples from the inside and outside surfaces. Undercooked tanks reach a maximum rate of degradation at a higher energy level than the ideal or overcooked tanks. In general, this supports the presence of more antioxidants in tanks subjected to shorter processing times (although the outside surface of the overcooked tank appears to degrade at a slightly higher energy level than the outside surface of the ideal tank). Time-to-Peak B values for all three tanks appear to be the same for samples from the inside surface, based on a P value of 0.91 and a corresponding probability of 9%. However, for samples from the outside surface, the difference between the time-to-Peak B values appears to be significant, with the overcooked tank reaching a peak at a slightly longer time followed by the undercooked and ideal tanks. Although there is no clear reason for longer times for the overcooked tanks, the broad degradation curves for the outside surfaces of the tanks could have led to some errors in estimating the time-to-Peak B values.

Comparison of results based on samples from inside and outside surfaces

Results depicted in Figures 12 and 13 allow for comparisons to be made between samples from the inside and outside surfaces of the tanks. Energy levels and time-to-peak values for Peak A and Peak B are shown

in Table IV for the inside and outside surfaces of the undercooked, ideal, and overcooked tanks. One-way ANOVAs are then performed to see if there are significant differences between values obtained for the inside and outside surfaces.

Probabilities of 94, 93, and 100% were obtained for ANOVAs that compared Peak A energy levels for samples from the inside and outside surfaces of the three tanks. Note that the Peak A energy level for the inside surface of the overcooked tank is significantly lower than the energy level for the outside surface of the tank. This trend is reversed for the undercooked and ideal tanks, with samples from the inside surface showing a significantly higher energy level at Peak A. Time-to-Peak A values also follow this same trend; however, the difference between values obtained for the inside and outside surfaces of the undercooked tank are not significant with a probability of only 23%. The reduction in Peak A energy level and shorter time-to-Peak A at the inside surface of the overcooked tank is consistent with the increased degradation and antioxidant consumption the tank experienced due to increased processing time. The inside surface of the overcooked tank is exposed to the air within the mold, which facilitates the oxidation process. In contrast, samples from the outside surfaces of the undercooked and ideal tanks degrade at lower Peak A energy levels than samples from the inside surfaces, and the time-to-Peak A is also shorter. This trend can be explained by noting that the layer at the outside surface is the first to be deposited on the mold wall and remains present on the metallic wall throughout the rotomolding process. Recall from eqs. (4) and (5) that alkoxy and peroxy radicals can be generated when hydroperoxides react with metal ions. These radicals can then participate in the chain propagation reaction shown in eq. (3), which leads to degradation of the polymer chains. This is a plausible explanation for the decreased Peak A energy levels for the outside surfaces of the undercooked and ideal tanks. These surfaces are in contact with the metallic mold wall and increased degradation occurs because of reactions between hydroperoxides and the metal ions. Note that air entrapped in the outside surfaces of the undercooked and ideal tanks can also play a role by initiating the formation of the hydroperoxides.

The trend discussed above for the Peak A energy levels measured for the undercooked and ideal tanks can also be observed in the Peak B energy levels. The Peak B energy levels for samples from the outside surfaces of these tanks are lower than the levels for samples from the inside surfaces with a high probability of 98% for the ideal tank, and a lower probability of 75% for the undercooked tank. Reactions between the metallic mold and the deposited polyethylene that forms the outside surface of the tank are believed to play a role. Note that the overcooked tank shows a similar trend for the Peak B energy levels. Unlike the Peak A levels, the Peak B levels for samples from the outside surface of the overcooked tank are lower than the levels for samples from the inside surface. Recall that the Peak B energy levels represent the maximum degradation rate for the polymer after antioxidants have been consumed, whereas Peak A represents the initial peak that occurs shortly after oxygen is introduced. [Peroxy radical and antioxidant radical generation occur according to eqs. (2) and (6) until Peak A is reached and the antioxidant radical levels are high enough to scavenge the peroxy radicals.] Therefore, Peak B energy levels provide a comparative measure of the maximum energy required to degrade the sample, and the lower energy level for the outside surface of the overcooked tank when compared to the inside surface can once again be explained by reactions between the deposited polymer and the metal mold walls. Last, time-to-Peak B values show some significant differences as evidenced by the 92% probability for samples from the undercooked tank. However, probabilities are lower for the ideal and overcooked tanks at 74 and 83%, and it is therefore difficult to make conclusive statements about the time-to-Peak B values for the inside versus the outside surfaces.

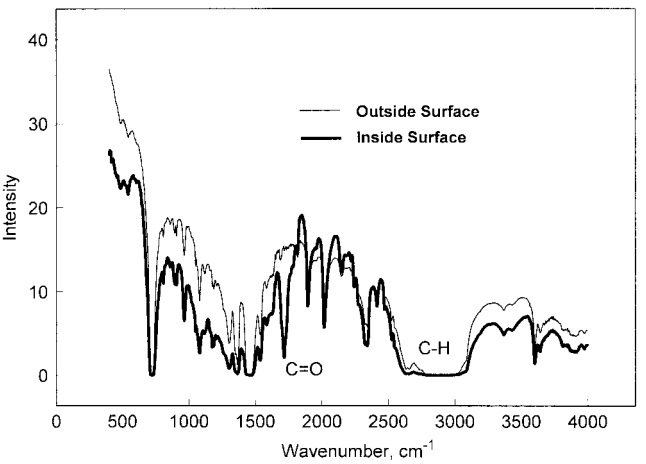

Figure 14 Fourier transfer infrared (FTIR) curves for samples from the inside and outside surfaces of the overcooked tank.

Chemical analysis and degradation products

Samples cut for FTIR measurements were taken from the inside and outside surfaces of the HDPE test tanks. Because the overcooked tank showed significant discoloring after processing, samples taken from the inside and outside surface of this tank were of particular interest. Results are presented in Figure 14. Absorption peaks present in these spectra indicate the presence of chemical groups, and the presence of peaks at certain wavenumbers is of greater significance than

the intensity of the peaks. Samples cut for the FTIR measurements had slightly different thicknesses; therefore, the intensities for the representative spectral peaks are different. The flat region between 2600 and 3100 cm^{-1} is indicative of the C—H groups, and they appear to be present in both the inside and the outside surface of the overcooked tank. Other peaks in the spectra are also present for both samples, with one exception. The carbonyl peak (C═O) is only present at the inside surface of the overcooked tank. This peak occurs at a wavenumber of 1720 cm^{-1}, and its presence is consistent with the formation of the quinone byproduct from the action of the antioxidants to inhibit free-radical formation in the HDPE material. It is also important to note that quinone compounds have a reddish or orange color to them, which is consistent with the discoloring of the inside surface of the tank.

Once Peak B is reached during the DSC-OIT experiments, all the samples show evidence of carbonyl generation as evidenced by the reddish color of the degraded sample. However, for samples from the inside surface of the overcooked tank, another quasi-stable end-product forms as shown by Peak B′ in Figure 11. For the samples that showed only a Peak B′ and no Peak B, the degraded sample was white rather than reddish in color. Because of the size of the sample, FTIR analysis could not be performed with available equipment. However, the degradation exhibited by Peak B′ could be indicative of the formation of another stable end-product such as the C—C coupled end-product discussed by Zweifel[9] and Pospisil and Nespurek.[11] These end-products do not contain the carbonyl groups in the aromatic ring and would not be reddish in color similar to the carbonyl-containing quinone end-products.

CONCLUSION

Three test tanks were rotomolded by using different total processing times to obtain undercooked, ideal, and overcooked tanks. DSC-OIT was used to study the degradation processes as well as FTIR. OIT measurements as defined by ASTM D3895 proved to be very short for all samples and occurred in less than 0.02 h. This showed that antioxidants were consumed during the rotomolding process because of scavenging of radicals. However, antioxidants were still present in the tanks after rotomolding, and the level of remaining antioxidants was different for the three tanks when comparisons were made by using samples from the inside and outside surfaces. The presence of antioxidants after rotomolding confirms that the material suppliers have blended appropriate levels of antioxidants with the polyethylene material.

By using numerically integrated data, Peak A energy levels for samples from the inside surface of the overcooked tank proved to be the lowest with short time-to-Peak A values. This corresponds with increased antioxidant and radical consumption during rotomolding of the overcooked tank, and lower antioxidant levels at the inside surface. FTIR results for samples from this surface confirmed the increased level of degradation after rotomolding because of excess carbonyl formation and quinone-type end-products. In comparison, Peak A energy levels and time-to-Peak A values for the ideal and undercooked tanks were higher than that measured for the overcooked tanks, which is consistent with the presence of more antioxidants in these tanks after processing. However, time-to-Peak A values for the undercooked tank proved to be shorter than that measured for the ideal tank, possibly due to the presence of entrapped air in the undercooked tank that could lead to radical generation and antioxidant consumption.

Statistical results for Peak A energy levels showed that processing time had a significant effect on residual antioxidant presence at the inside surface of the rotomolded tanks, whereas processing time had a less significant effect on residual antioxidant presence at the outside surface. Peak B energy levels for samples from the inside surfaces of the three tanks supported this conclusion with the undercooked and ideal tank samples reaching a maximum degradation rate at a higher energy level than the overcooked tank samples.

By using samples from the inside and outside surfaces of each tank, the effects of exposure to the heated metal mold wall could be observed in addition to the effects of being exposed to the hot air inside the mold. Only the inside surface of the overcooked tank had lower Peak A energy levels and corresponding shorter time-to-Peak A values when compared to samples from the outside surface of the overcooked tank. This is once again due to increased consumption of antioxidants during the rotomolding process. However, samples from the inside surfaces of the undercooked and ideal tanks showed higher Peak A energy levels and time-to-Peak A values than samples from the outside surfaces of these tanks. This could be attributed to increased degradation from the outside surfaces being in contact with the heated metal mold wall. Metal ions could have led to an increase in alkoxy and peroxy radicals that contributed to degradation of the polyethylene material. A similar trend was observed for Peak B energy levels when samples from the inside and outside surfaces of the undercooked and ideal tank were compared.

From these results, rotomolders can observe that antioxidants will not only be present in their thick-walled polyethylene products after processing, but the level of antioxidants will be different at the inside and outside surfaces. Results also show that the level of residual antioxidants is a function of processing time. Therefore, rotomolders need to make sure that the ideal processing times are fol-

lowed to ensure that their products are able to withstand oxidation from long-term exposure to chemicals and the environment.

The authors acknowledge Professors P. Jones and D. Wedegaertner at the University of the Pacific for assistance with the FTIR experiments. They also acknowledge Keith Foster of Poly Processing, who rotomolded the sample tanks used in the study.

References

1. Crawford, R. J., Ed., Rotational Moulding of Plastics, 2nd ed.; Wiley: New York, 1996.
2. Nugent, P. Rotational Molding: A Practical Guide; Paul: Reading, PA, 2001.
3. Cramez, M. C.; Oliveira, M. J.; Crawford, R. J. Polym Degrad Stab 2002, 75, 321–327.
4. Gugumus, F. in Plastics Additives Handbook, 3rd ed.; Gachter, R.; Muller, H., Eds., Hanser: New York, 1990.
5. Schwarzenbach, K.; Gilg, B.; Muller, D.; Knobloch, G.; Pauquet, J. R.; Rota-Graziosi, P.; Schmitter, A.; Zingg, J.; Kramer, E. in Plastics Additive Handbook, 5th ed.; Zweifel, H., Ed., Hanser Gardner Publishers: Cincinnati, OH, 2001; Chapter 1.
6. Pauqet, J. R.; Todesco, R. V.; Drake, W. O. Int Wire Cable Symp 1993, 0, 77.
7. Riga, A.; Patterson, G., Eds. Oxidative Behavior of Materials by Thermal Analytical Techniques; ASTM Special Technical Publication STP1326; ASTM 1997.
8. Rosa, D. S.; Sarti, J.; Mei, L. H. I.; Filho, M. M.; Silveira, S. Polym Testing 2000, 19, 523.
9. Zweifel, H. Stabilization of Polymeric Materials; Springer-Verlag: New York, 1998.
10. Shylapnikov, Y. A.; Kiryushkin, S. G.; Mar'in, A. P. Antioxidative Stabilization of Polymers; Taylor & Francis: Bristol, PA, 1996.
11. Pospisil, J.; Nespurek, S. in Handbook of Polymer Degradation, 2nd ed.; Hamid, H., Ed.; Marcel Dekker: New York, 2000; Chapter 6.